Available online at www.sciencedirect.com

ScienceDirect

Procedia Structural Integrity 2 (2016) 3508–3514

Structural Integrity Procedia

www.elsevier.com/locate/procedia

21st European Conference on Fracture, ECF21, 20-24 June 2016, Catania, Italy

# Weldability of austenitic stainless steel by metal arc welding with different shielding gas

Girolamo Costanza[a*], Andrea Sili[b], Maria Elisa Tata[a]

[a] *Dipartimento di Ingegneria Industriale, Università di Roma-Tor Vergata, Via del Politecnico 1, 00133 Roma - Italy*
[b] *Dipartimento di Ingegneria, Università di Messina, 98166 Messina- Italy*

**Abstract**

During fusion welding the molten metal is shielded from contact with the atmospheric gas by means of a gaseous flux. The shielding gas prevents weld embrittlement, affects welding quality, because of its influence on filler metal transfer, and has a direct impact on welding costs as well. Argon is the most common shielding gas, often used with some adds of other gases that can be inert, as helium, or active, as $CO_2$, $O_2$ or $H_2$. In this work the effects of mixtures with different composition have been considered for the arc welding of austenitic steels. Metallographic samples of welded sections have been undergone to visual and optical microscopy observations, microhardness, indentations and tensile tests.


Peer-review under responsibility of the Scientific Committee of ECF21.

Keywords: austenitic steel, GTAW, GMAW, shielding gas, joint efficiency

## 1. Introduction

Gas Metal Arc Welding (GMAW) is widely used in industry, thanks to its peculiar characteristics such as high production rates, easiness of automation and ability to obtain high quality welds with many metals. Gas Tungsten Arc Welding (GTAW) can be employed to manufacture high quality joints in a variety of materials, but it does not find wide applications in thick components due to its poor productivity. In arc welding process parameters as current, voltage, polarity, electrode diameter, shielding gas composition and flow rate have all a great influence to perform a successful welds. In particular the way the molten metal is transferred from the electrode to the workpiece affects the arc stability and the chance of having sound welds with good penetration and bead morphology. Many researchers addressed their interest to study in GMAW the filler transfer modes and their consequence for the weldabilty (Wang et al. 2003 and Cuiuri et al. 2002) and in the case of GTAW the way of supplying shielding gas

* Corresponding author. Tel.: +39 06 72597185
*E-mail address:* costanza@ing.uniroma2.it


Peer review under responsibility of the Scientific Committee of ECF21.
10.1016/j.prostr.2016.06.437

was also considered (Kim et al. 2006) and in the comparison of SMAW-GTAW techniques with different welding parameters (Barbieri et al. 2015).

**Nomenclature**

| | |
|---|---|
| F | load recorded during FIMEC test |
| p | specific pressure in FIMEC test |
| $p_L$ | specific pressure at the beginning of the plastic deformation linear stage |
| $p_y$ | specific pressure at the end of the plastic deformation linear stage |
| r | cylinder indenter radius |
| x | distance from welding axis measured on the welded sections |
| $\delta$ | penetration depth recorded during FIMEC test |
| $\sigma_y$ | yield stress obtained by tensile test |
| $\sigma_u$ | ultimate stress obtained by tensile test |
| $\eta$ | joint efficiency |

In general the use of a gaseous flux to shield molten metal from contact with the atmospheric oxygen and nitrogen, which cause defects and porosity, is necessary to prevent joint embrittlement. Moreover current operating parameters and shielding gas composition affect welding quality, because of their influence on filler metal transfer mode (Hu et al. 2007), having a direct impact on welding costs as well (Rao et. al. 2010). In general a gas with high thermal conductivity produce the hottest and most fluid weld puddle, while some adds of an oxidizing gas reduces surface tension enhancing wetting of weld bead to base material.

Argon is considered the basic shielding gas. Helium can be added to increase penetration and fluidity of the weld pool, small additions of oxygen or carbon dioxide are usually needed to stabilize the arc, improve fluidity and bead quality. The use of mixtures of inert gas, as argon, results in higher level of wire electrode deposit and welding speeds. For welding austenitic stainless steels the addition of small amounts of hydrogen gives similar, but much stronger effects than helium; however hydrogen must be avoided to weld martensitic, ferritic or duplex grades.

In this paper the effects of various shielding gases on weldability of AISI 304 and AISI 316 austenitic stainless steels are considered. Commercial mixtures of Ar, with different percentage of He, $CO_2$ and $H_2$, were experimented in order to obtain sound welds. Metallographic samples of the welded sections have been characterized by optical microscopy observations.

Residual stress, microstructural and metallurgical modifications are extremely important in welds (Bonaccorsi et. al. 2012, Missori et al. 2008 and Missori et al. 2015). In this work bulk mechanical strength of parent metal and welds were experimented by tensile tests. Because the homogeneity of mechanical properties is a basic condition in welds to avoids premature failure, Vickers microhardness surveys were carried out across the welded sections to check any metallurgical changes in the heat affected zone (HAZ), which could lead to local hardening and embrittlement. Moreover mechanical properties of base metal (BM) and welded zone (WZ) were investigated by means of the instrumented indentation test FIMEC (Flat-top cylinder Indenter for MEchanical Characterization), that is able to estimate the yield stress in a small portion of material (Donato et al. 1998, Calogero et al. 2014).

## 2. Materials and methods

Shielding gases (see for their classification the AWS/ANSI code quoted in the References) are primary utilized for molten pool protection against atmospheric gas, including oxygen, nitrogen and hydrogen, because the reaction with molten metal gives rise to many problems (oxide inclusion, hydrogen diffusion, porosity), leading to welds embrittlement.

Shielding gas also plays an important role in determining weld penetration profiles, helping to maintain arc stability and achieving the desired mechanical properties in welds. Moreover shielding gas affects the filler metal transfer mechanism, which in turns contributes to process efficiency and bead appearance (Mukhopadhyay et al. 2013).

Argon is an inert gas useful for butt welds because it produces narrow penetration profiles. Pure argon is commonly used due to the stable arc features.

Helium performs a 'hotter' arc that allows faster welding speeds and consequently higher production rates. However, helium is very expensive and requires higher flow rates than argon, so any productivity increment has to be balanced with the increased cost for shielding gas. Because helium produces a wide, deep penetration profile, it works well with thick materials, usually together with about 75% of argon.

Carbon dioxide is the least expensive of the shielding gases so it is an attractive choice when costs are the main priority. Pure $CO_2$ provides very deep weld penetration, but produces a less stable arc and more spatter than a mixture with other gases. Therefore Ar with some percents of $CO_2$ gives a good combination of arc stability, puddle control, reducing spatter as well, related to a correct choice of current operating condition as pointed out by Soderstrom et al. and Boiko et al (2008).

Hydrogen increases the heat supplied to the base metal. Adds of 2-5% of hydrogen to argon allow to obtain welding speeds comparable to the ones performed with pure argon. These mixtures are used in automated welding of stainless steel.

Oxygen is a reactive gas that can be very dangerous for molten metal, but limited adds to argon helps to improve weld pool fluidity, weld penetration and arc stability, particularly when welding carbon, low alloy or stainless steels (Pires et al. 2007). It is not recommended in the case of oxidizable metals as aluminum, magnesium or copper. In a previous work (Bonaccorsi et al. 2011) laser beam welded carbon steel plates, clad with high alloyed metals, have been manufactured with Ni alloys as filler metal and characterized. Such steels are an economical solution to meet the increasing demand of chip materials that combine good mechanical and corrosion resistance properties.

In this work welding trials on AISI 304 and 316 plates (3 mm thick) were performed with the aim of testing the effect of different shielding gas. Plates were butt-welded with beveled preparation (V groove and bevel angle of 60°). GTAW and GMAW were performed respectively by means of Miller model Syncrowave 275 P and WECO model Discovery 351 MSW welding machines. Wires of AISI 308 and 316 were utilized as filler materials for welding AISI 304 and 316 respectively.

Samples for metallographic observations and microhardness tests were prepared by cutting welds normally to the welding direction. These samples were first mechanical polished and then chemical etched with glyceregia type solution (20 ml $HNO_3$, 60 ml HCl, 40 ml glycerine).

Table 1 shows welding procedure, shielding gas composition and material for each sample considered in our experiments.

Table 1 - Samples, materials, welding procedures and shielding gas.

| Sample No | Sample material | Welding procedure | Shielding gas | Gas composition |
|---|---|---|---|---|
| 1 | AISI 304 | GTAW | Hydrostar H2 | 98%Ar, 2%$H_2$ |
| 2 | AISI 316 | GTAW | Hydrostar H2 | " " |
| 3 | AISI 304 | GTAW | Hydrostar H5 | 95%Ar, 5%$H_2$ |
| 4 | AISI 304 | GTAW | Hydrostar T300 | 75%Ar,20%He,5%$H_2$ |
| 5 | AISI 304 | GMAW | Hydrostar PB | 95%Ar,4%$CO_2$,1%$H_2$ |
| 6 | AISI 304 | GTAW | Argon | 100%Ar |
| 7 | AISI 316 | GTAW | Argon | 100%Ar |
| 8 | AISI 304 | GMAW | Stargon C2 | 90%Ar,8%$CO_2$,2%$O_2$ |

Vickers microhardness tests were carried out on metallographic samples along a line transversally to the welding axis. The test load was 300 g applied for 10s.

Tensile test were performed on sheets of both parent metal and welds, in order to investigate mechanical and metallurgical modifications occurring in steel welds. Specimens were 80 mm long, 15 mm wide and 3 mm thick (initial resistant section of 45 $mm^2$). They were milled in order to have smooth surfaces.

FIMEC indentation tests were carried out with a cylindrical probe (radius r = 0.5 mm) at an advancing speed of 0.1 mm/min on the welded zones of the different samples and for comparison on the base materials. During FIMEC test, load values (F) were recorded and then plotted as a function of penetration depth. The specific pressure (p) was calculated as load / probe area ratio.

## 3. Results and discussion

The quality of welding is considered acceptable when the deposit has adequate penetration, right bead profile and absence of external and internal defects. In our experiments all the welded samples have exhibited a satisfactory macrographic appearance with full penetration, almost regular geometry and no visible macroscopic defects (fig. 1).

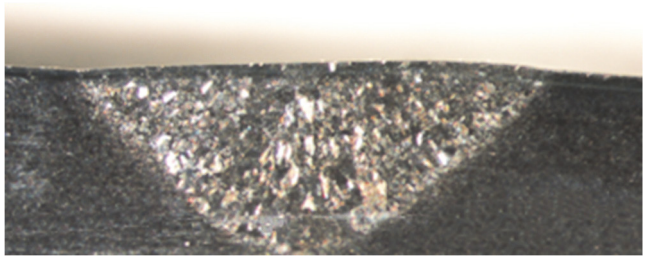

Fig. 1 - Macrograph of a welded section (samples 1).

The two base steels, AISI 304 and 316, have both a fine microstructure with average grain size around 20 μm (see figure 2a). The WZ of the various samples is characterized by solidification structures that follows the thermal flux directions (see figures 2b and 2c).

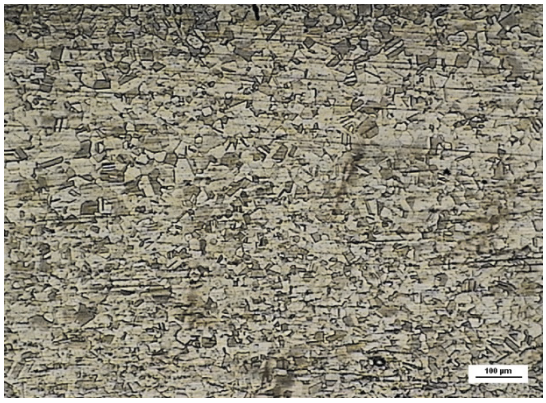


a)


b)


c)

Fig. 2 - Micrograph of metallographic samples: AISI 304 base material (a), ZTA (b) and WZ (c) of sample 5.

Results of microhardness tests are plotted vs. the distance (x) from the welding axis, as shown in figure 3 for a representative case. The HAZ is clear recognizable being characterized by higher microhardness values and in some case by peaks. Microhardness values are summarized in table 2. Both microhardness values of AISI 304 and 316 base metals are around 160 HV; in the welded zones of the various samples significantly higher values have been recorded. The higher hardness values recorded in the HAZ can be ascribed to chromium carbide precipitation phenomena due to the welding thermal cycle.

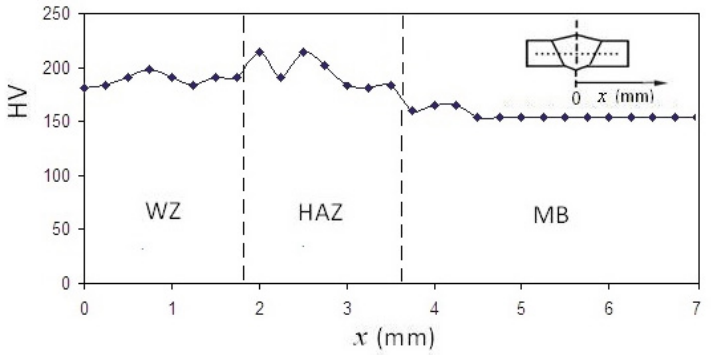


Fig. 3 – Vickers microhardness values vs. distance from welding axis (sample 2).

Table 2 - Results of Vickers microhardness test.

| Sample No | Sample material | Hardness (BM) | Hardness (HAZ) | Hardness (WZ) |
|---|---|---|---|---|
| 1 | AISI 304 | 155 | 155-175 | 155-175 |
| 2 | AISI 316 | 155 | 180-213 | 180-200 |
| 3 | AISI 304 | 165 | 160-201 | 155-177 |
| 4 | AISI 304 | 155 | 170-209 | 165-190 |
| 5 | AISI 304 | 155 | 155-170 | 155-165 |
| 6 | AISI 304 | 165 | 160-183 | 160-172 |
| 7 | AISI 316 | 155 | 165-209 | 177-187 |
| 8 | AISI 304 | 165 | 160-205 | 162-183 |

As it can be found in literature for a wide number of metals and alloys (see the works of Donato et al. 1998, Riccardi et al. 2001, Filacchioni et al. 2004), the load (F) vs. penetration depth (δ) diagrams obtained by FIMEC test are characterized by an initial elastic stage until a specific pressure ($p_L$) is reached, followed by a plastic deformation stage with a linear trend up to a pressure ($p_y$), where larger plastic deformation starts with a sharp variation of slope (here a protrusion of material occurs around the indentation), and then by an almost constant slope deformation stage with a remarkable plastic flow. Fig. 4 shows the load vs. penetration depth diagram for sample 1.

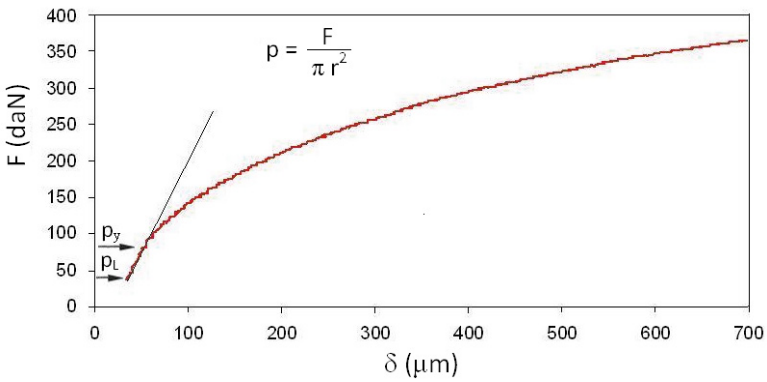


Fig. 4 – Diagram load - penetration depth recorded during FIMEC test on welded zone (sample 1).

When penetration rate does not exceed 0.1 mm/min, FIMEC test gives good indications about mechanical behavior of materials during tensile test with deformation rate of $10^{-3}$ $s^{-1}$. In these conditions the following relationship has been experimented to estimate the yield strength $\sigma_y$ through the pressure $p_y$:

$$\sigma_y \approx p_y/3 \quad (1)$$

The $p_y/3$ values, obtained by FIMEC test performed on base materials and welded zones of the various samples, are given in table 3.

Table 3 - Results of FIMEC test.

| Sample No | Sample material | Test zone | $p_y/3$ (MPa) |
|---|---|---|---|
| | AISI 304 | BM | 339 |
| | AISI 316 | BM | 339 |
| 1 | AISI 304 | WZ | 280 |
| 2 | AISI 316 | WZ | 290 |
| 3 | AISI 304 | WZ | 310 |
| 4 | AISI 304 | WZ | 310 |
| 5 | AISI 304 | WZ | 278 |
| 6 | AISI 304 | WZ | 289 |
| 7 | AISI 316 | WZ | 275 |
| 8 | AISI 304 | WZ | 279 |

Table 4 - Results of tensile test: yield stress and joint efficiency.

| Sample No | Sample material | $\sigma_y$ (MPa) | Fracture zone | Joint efficiency (%) |
|---|---|---|---|---|
| | AISI 304 (parent metal) | 335 | | |
| | AISI 316 (parent metal) | 312 | | |
| 1 | AISI 304 | 280 | WZ | 83 |
| 2 | AISI 316 | 290 | WZ | 93 |
| 3 | AISI 304 | 300 | WZ | 89 |
| 4 | AISI 304 | 310 | WZ | 92 |
| 5 | AISI 304 | 270 | WZ | 80 |
| 6 | AISI 304 | 270 | WZ | 80 |
| 7 | AISI 316 | 275 | WZ | 88 |
| 8 | AISI 304 | 288 | WZ | 86 |

Table 5 - Results of tensile test: ultimate stress and joint efficiency.

| Sample No | Sample material | $\sigma_u$ (MPa) | Fracture zone | Joint efficiency (%) |
|---|---|---|---|---|
| | AISI 304 (parent metal) | 714 | | |
| | AISI 316 (parent metal) | 625 | | |
| 1 | AISI 304 | 606 | WZ | 85 |
| 2 | AISI 316 | 569 | WZ | 91 |
| 3 | AISI 304 | 594 | WZ | 83 |
| 4 | AISI 304 | 618 | WZ | 87 |
| 5 | AISI 304 | 578 | WZ | 81 |
| 6 | AISI 304 | 616 | WZ | 86 |
| 7 | AISI 316 | 571 | WZ | 91 |
| 8 | AISI 304 | 589 | WZ | 83 |

During tensile test all the samples have shown plastic behavior with large deformations and final fracture localized in the WZ. Moreover it is worth to notice that the yield stress of each sample is very close to the $p_y/3$ value obtained by FIMEC test. Yield and ultimate stress data are given respectively in table 4 and 5, together with the joint

efficiency (η) values calculated by the following ratio:

$$\eta = \text{strength of weld / strength of parent metal} \quad (2)$$

## 4. Conclusions

The AISI 304 and 316 sheets have shown a good weldability utilizing the electric arc and different compositions of the shielding gas (pure Ar or Ar plus He, $H_2$, $CO_2$ or $O_2$). Satisfactory macrographic appearance with good penetration, right bead profile and absence of macroscopic defects has been observed. Metallographic investigation on welded sections have shown the typical solidification structures and Vickers microhardness tests have assessed the presence of hardened heat affected zones. As regard the homogeneity of the microhardness profile across the welded sections, the best results have been obtained in the AISI 304 plates welded with Hydrostar H2, Hydrostar PB or pure argon as shielding gas (respectively samples 1, 5 and 6) which maintain hardness values not so different from the base material ones; while in the other cases microhardeness peaks around 200 HV are reached. The welded zone is characterized by some lack of mechanical strength as pointed out by FIMEC and tensile test. In any case the joint efficiency results very high, particularly for AISI 316 plates welded with Hydrostar H2 or pure argon (respectively samples 2 and 7), where the efficiency achieves values around 90% for the ultimate stress.

## References


ANSI / AWS A5.32/A5.32M - 97 (R2007). Specification for Welding Shielding Gases. Approved by the American National Standards Institute, 8, 1997

Barbieri G., Cesaroni M., Ciambella L., Costanza G, Montanari R., 2015. Influence of welding parameters on microstructure of welded joints SMAW/GTAW steel X10 CrMoVNb 9-1 (P91). Metallurgia Italiana 107(3), 37-45.

Boiko I., Avisans D., 2013. Study of Shielding Gases for MAG Welding. Materials Physics and Mechanics 16, 126-134.

Bonaccorsi L., Costanza G., Missori S., Sili A., Tata M.E., 2012. Mechanical and metallurgical characterization of 8090 Al-Li alloy welded joints. Metallurgist, 56(1-2), 75-84.

Bonaccorsi L., Costanza G., Giacobbe F., Missori S., Sili A., Tata M.E., 2011. Laser beam welding of Ni alloy-clad steel plates. Metallurgia Italiana 5, 43-51.

Calogero V., Costanza G., Missori S., Sili A., Tata M.E., 2014. A weldability study of Al-Cu-Li 2198 alloy. Metallurgist, 57(11-12), 1.134-1.141.

Cuiuri D., Norrish J., Cook C., 2002. New Approaches to Controlling Unstable Gas Metal Arc. Welding. Australasian Welding Journal 47(3), 39–47.

Donato A., Gondi P., Montanari R., Moreschi, Sili A. and Storai S., 1998. A Remotely Operated FIMEC Apparatus for the Mechanical Characterization of Neutron Irradiated Materials. Journal of Nuclear Materials, 258-263, 446-451.

Filacchioni G., Montanari R., Riccardi B., Tata M. E., Costanza G., 2004. Characterisation of EUROFER-97 TIG welded joints by indentation tests (FIMEC). Journal of Nuclear Materials 329-333, 1529-1533.

Hu J., Tsai H.L., 2007. Heat and Mass transfer in Gas Metal Arc Welding. Part I: the Arc. International Journal of Heat and Mass Transfer, 50, 833–846.

Hu J., Tsai H.L., 2007. Heat and Mass transfer in Gas Metal Arc Welding. Part II: the Metal. International Journal of Heat and Mass Transfer, 50, 808–820.

Kim I.S., Son J.S., Kim H.J., Chin B.A., 2006. Development of a Mathematical Model to Study on Variation of Shielding Gas in GTA Welding. Journal of Achievements in Materials and Manufacturing Engineering, 19 (2), 73-80.

Missori S., Tata M.E., Costanza G., Sili A., 2008. Microstructural transformations on quenched and tempered ASA CA 80 steel welds. Proceedings of International Conference New Developments on Metallurgy and Applications of High Strength Steels, Buenos Aires, 2008.

Missori S., Costanza G., Sili A., Tata M.E., 2015. Metallurgical modifications and residual stress in welded steel with average carbon content. Welding International, 29(2), 124-130.

Mukhopadhyay S., Pal T.K., 2006. Effect of Shielding Gas Mixture on Gas Metal Arc Welding of HSLA Steel Using Solid and Flux Cored Wires. International Journal Advanced Technology, 29, 262-268.

Mukhopadhyay P., Chattopadhyaya S., Bhatia S., Singh N.K., 2013. Prediction of Weld Parameters in Gas Metal Arc Welding Process Using Curve Fitting techniques and graphical methods. Advanced Materials Research, 652-654, 2352-2356.

Pires I., Quintino L., Miranda R.M., 2007. Analysis of the influence of shielding gas mixtures on the gas metal arc welding metal transfer modes and fume formation rate. Materials and Design, 28 (5), 1623-1631.

Rao Z.H., Hu J., Liao S.M., Tsai H.L., 2010. Modeling of the transport phenomena in GMAW using argon–helium mixtures. Part I – The arc. International Journal of Heat and Mass Transfer, 53, 5707–5721.

Rao Z.H., Hu J., Liao S.M., Tsai H.L., 2010. Modeling of the transport phenomena in GMAW using argon–helium mixtures. Part II – The metal. International Journal of Heat and Mass Transfer 53, 5722–5732.

Riccardi B., Montanari R., Moreschi L. F., Sili A., Storai S., 2001. Mechanical Characterisation of Fusion Materials by Indentation Test. Fusion Engineering and Design, 58-59, 755-759.

Soderstrom E. J., Mendez P.F., 2008. Metal Transfer during GMAW with Thin Electrodes and Ar-$CO_2$ Shielding Gas Mixtures. Welding Journal, 87, 124s-133s.

Wang G., Huang P.G., Zhang Y.M., 2003. Numerical Analysis of Metal Transfer in Gas Metal Arc Welding. Metallurgical and Materials Transactions, B 34B, 345–353.